PHYSICAL REVIEW B **86**, 041302(R) (2012)

Time-resolved photoluminescence spectroscopy of individual GaN nanowires

A. Gorgis, T. Flissikowski,* O. Brandt, C. Chèze, L. Geelhaar, H. Riechert, and H. T. Grahn
Paul-Drude-Institut für Festkörperelektronik, Hausvogteiplatz 5-7, 10117 Berlin, Germany
(Received 27 March 2012; published 30 July 2012)

We investigate individual and ensembles of free-standing GaN nanowires (NWs) grown by plasma-assisted molecular beam epitaxy using time-resolved photoluminescence (TRPL) spectroscopy. The PL transients of individual NWs always show a single exponential decay, independent of the excitation density. However, different NWs exhibit different decay times ranging from about 50 to 400 ps. In contrast, the PL transients of the NW ensemble always exhibit a nonexponential decay even at low excitation densities. We conclude that this nonexponential PL decay of the NW ensemble is a superposition of the different decay times of the different individual NWs in the ensemble. The origin of these different decay times is attributed to the impact of surface recombination.

DOI: 10.1103/PhysRevB.86.041302 PACS number(s): 78.47.jd, 78.67.Uh, 78.55.−m, 71.35.−y

GaN nanowires (NWs) can be synthesized in high structural quality even on foreign substrates, in contrast to conventional heteroepitaxial GaN films. In combination with (In,Ga)N, they thus may result in cost-efficient implementations for light-emitting diodes (LEDs) in the blue and green spectral range,[1–3] chemical and gas sensing devices,[4,5] and photovoltaic applications.[6] Most of these applications require a large number of NWs, i.e., NW ensembles. However, NW ensembles always consist of a large number of individual NWs, which exhibit different properties due to different lengths, diameters, and shapes because of random nucleation processes and local fluctuations in the growth parameters.[7] Furthermore, the number of impurities in an individual NW and their location within the NW vary according to Poisson statistics.[8] Consequently, the response from the NW ensemble is composed of an average of the responses from the individual NWs within the ensemble. In Ref. 8, we pointed out that this averaging effect can mask fundamental information concerning the energy level structure of individual NWs. For a better understanding of the properties of the NW ensemble, detailed investigations of individual NWs are therefore necessary. In the previous study presented in Ref. 8, several hundred photoluminescence (PL) spectra from different free-standing individual NWs were statistically analyzed, including the intensity, the energy, and the origin of the PL lines, demonstrating the individual character of each NW. In this way, we have obtained an insight into the recombination channels active in individual NWs, but information about the corresponding *recombination dynamics* is still lacking.

To obtain information on the recombination dynamics, the measurement of the decay time τ (or recombination rate $1/\tau = \gamma$) of individual NWs using time-resolved photoluminescence (TRPL) spectroscopy is required. An average value of τ can be retrieved from the PL transients of a NW ensemble.[9] However, because individual NWs exhibit different recombination channels, in particular due to a varying influence of the surface, the functional time dependence of the PL decay of the NW ensemble can be hardly understood without knowledge of the PL transients of the individual NWs. The experimental challenge of TRPL spectroscopy on individual NWs is the measurement of PL transients with a dynamic range of several orders of magnitude. Furthermore, the properties of individual NWs should not be altered by any processing steps necessary to enable the selection of a single NW.

In the present Rapid Communication, we report an investigation of the decay time of individual NWs with a volume of less than 2×10^{-16} cm^3 using time-correlated single-photon counting in connection with a setup for TRPL spectroscopy with a spatial resolution of a few μm, which enables us to determine τ for individual free-standing NWs. We compare the PL transients of single NWs with data recorded on the NW ensemble, where the PL signal of about 1500 NWs is collected. In both cases, the PL signal is dominated by the donor-bound exciton (D^0, X_A) and the free exciton (X_A).

The investigated NWs were grown by plasma-assisted molecular beam epitaxy on a Si(111) substrate. By selecting appropriate growth conditions, self-induced, i.e., catalyst-free, NW growth was possible preventing the introduction of impurities into the NWs by catalyst elements. Detailed information on the growth of the investigated GaN NWs can be found elsewhere.[7] For the investigations presented in this Rapid Communication, we use the same sample as in Ref. 8.

The NW density as well as the diameter and length of the NWs are important parameters for our investigations. Therefore, the NWs have also been investigated by scanning electron microscopy (SEM). Due to the influence of the electron beam on the optical characteristics, most of the SEM images were recorded after the optical experiments were performed or at positions, where no optical spectra or transients were recorded. Figures 1(a) and 1(b) show typical images of the central part of the NW wafer. In this region, the NWs are uniformly distributed with a density of about 100 μm^{-2}, an average diameter of about 50 nm, and a length up to 400 nm. Closer to the edge of the NW wafer, the conditions during growth are different from the ones in the central part of the NW wafer. The substrate temperature is slightly higher, which results in significantly reduced nucleation probability. The SEM images in Figs. 1(c) and 1(d) clearly show that the diameter and the length of the NWs are drastically reduced and that the NW density is much smaller in this region. Very close to the edge, we can even find locations as shown in Figs. 1(e) and 1(f), where the NW density is so small that a single free-standing or chipped-off NW, respectively, can be easily addressed within the resolution of an optical

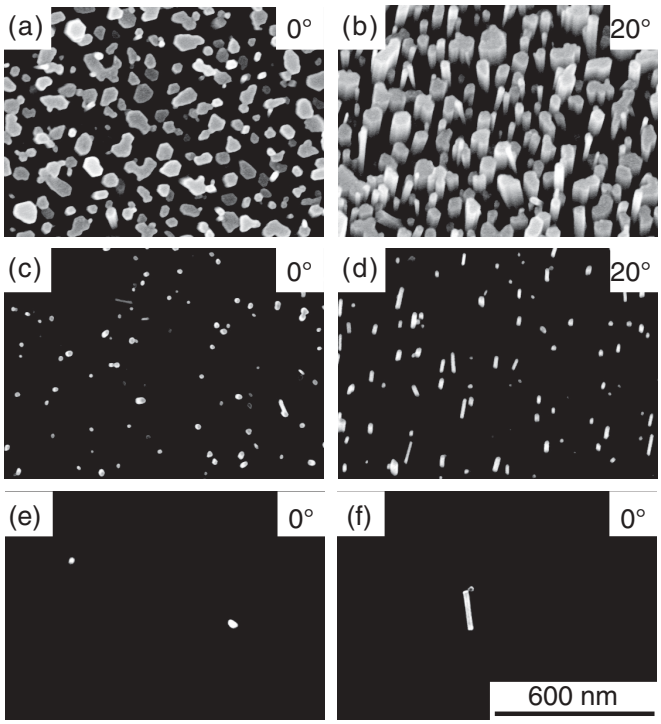

FIG. 1. SEM images of GaN NWs in the central part of the wafer in (a) top view (angle of incidence $\phi = 0°$) and (b) bird's-eye view ($\phi = 20°$). (c) and (d) are respective SEM images recorded closer to the edge of the wafer. (e) and (f) are top-view images of a free-standing and a chipped-off NW, respectively, very close to the edge of the wafer. The density and diameter of the NWs are clearly reduced from the center to the edge of the wafer.

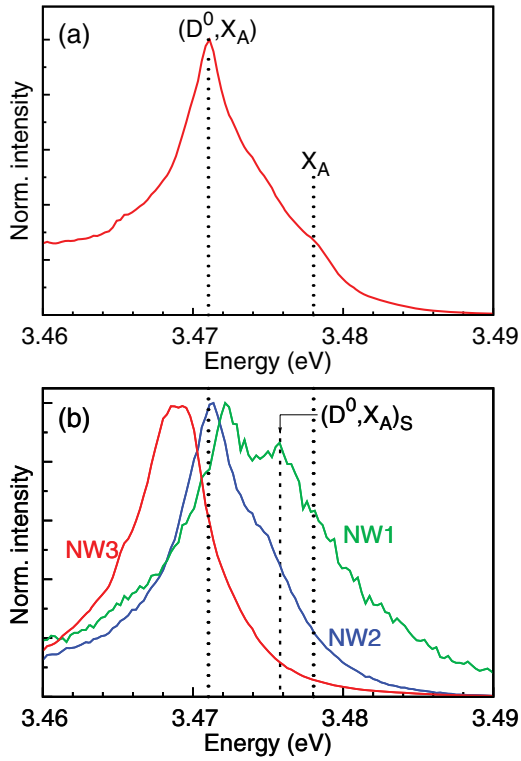

FIG. 2. (Color online) Time-integrated PL spectra for (a) an ensemble of about 1500 GaN NWs and (b) three individual GaN NWs labeled NW1, NW2, and NW3 recorded at 5 K for pulsed excitation. The dotted lines in (a) and (b) at 3.471 and 3.478 eV indicate the energy of the (D^0, X_A) and X_A line, respectively, in unstrained GaN. The dashed line in (b) denotes the energy of a $(D^0, X_A)_S$ exciton.

microscope. In this region, the largest NWs exhibit a diameter of about 30 nm with a length of about 300 nm, resulting in a total volume of 2×10^{-16} cm^3. The low density of the NWs in this region offers the possibility to investigate the decay times of individual, free-standing NWs, which are not altered by strain or solvents as may be the case for dispersed NWs.

For the TRPL investigations of single NWs, a sufficient spatial resolution on the one hand and a long-term stability on the other hand are required in order to obtain reliable information. In order to achieve the necessary stability, the samples were placed in a microscope cryostat, which can be cooled down to temperatures of about 5 K and which is directly mounted onto the optical table. The spatial resolution was provided by a microscope objective with a long working distance and a magnification of 20. We used a confocal arrangement, i.e., the excitation laser was focused, and the resulting PL signal was detected by the same microscope objective.

In all measurements of the PL spectra and of the PL transients, the samples were excited by the second harmonic of pulses obtained from an optical parametric oscillator (APE OPO PP Automatic) synchronously pumped by a femtosecond Ti:sapphire laser (Coherent Mira 900), which itself was pumped by a frequency-doubled Nd:vanadate continuous-wave laser (Coherent Verdi V 10). The pulse length after the optical parametric oscillator was about 200 fs. The employed wavelength was 325 nm, and the repetition rate of the laser system was 76 MHz. The spot size of the laser beam on the sample surface was about 3×11 μm^2 with a maximum energy fluence ρ_E of 37 μJ cm^{-2} for a single laser pulse. In order to detect the PL signal with a higher spatial resolution than the size of the laser spot, we introduced a pinhole with a 50 μm diameter directly in front of the detection system. Together with a virtual image of the sample surface, only light coming from a specific area inside the excitation spot entered the detection system. Altogether, we achieved a spatial resolution of the detected signal of 5 μm diameter with a drift stability of a few μm sufficient for typical integration times. After the pinhole, the PL signal was dispersed by a spectrometer with a spectral resolution of 0.2 nm and detected by a liquid-nitrogen-cooled CCD camera in order to record time-integrated spectra. For the TRPL experiments, the second exit of the spectrometer was equipped with a microchannel plate photomultiplier tube (MCP-PMT, Hamamatsu Photonics R3809U-50). The MCP-PMT, together with a time-correlated single-photon counting (TCSPC) system (PicoQuant PicoHarp 300), was used to record the PL transients integrated over a specific energy range with a time resolution of about 35 ps.

Figure 2(a) displays a time-integrated PL spectrum of the NW ensemble from about 1500 NWs measured in the central part of the NW wafer. At low temperatures, the spectrum is dominated by the PL line of the donor-bound exciton (D^0, X_A) at 3.471 eV. The PL line of the free exciton X_A is visible as a shoulder at 3.478 eV. The energies for the (D^0, X_A) and the X_A line indicated by the dotted lines in Fig. 2(a) are in excellent

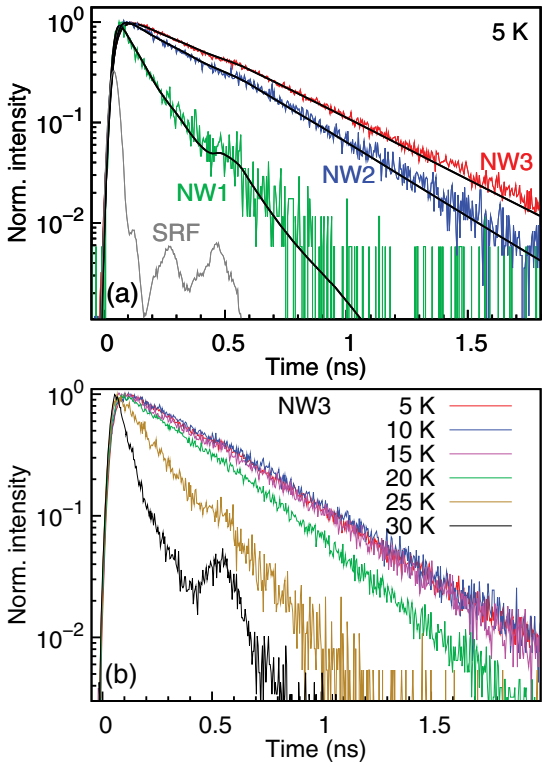

FIG. 3. (Color) (a) PL transients of three different individual GaN NWs labeled NW1 (green line), NW2 (blue line), and NW3 (red line) and corresponding single exponential fits (black lines) convoluted with the SRF (gray line) at 5 K. All three transients have been recorded by integrating spectrally over the whole PL line of the corresponding NW. (b) PL transients of NW3 for different temperatures of 5 (red), 10 (blue), 15 (magenta), 20 (green), 25 (dark yellow), and 30 K (black).

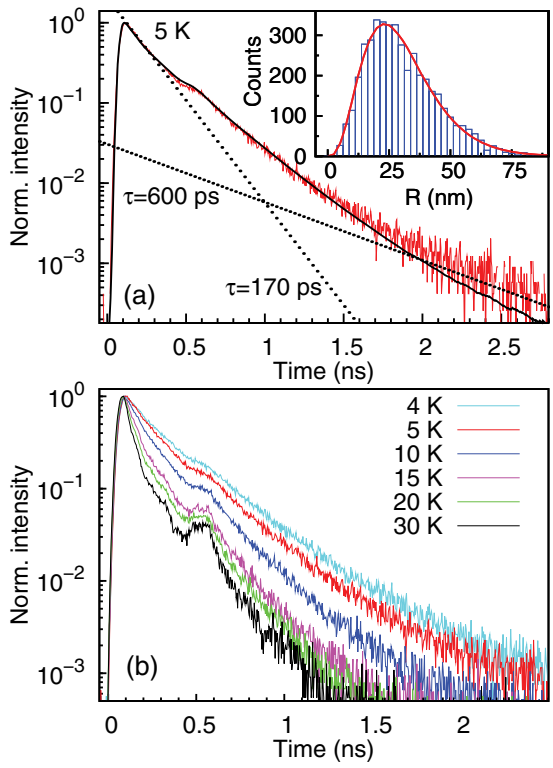

FIG. 4. (Color) (a) PL transient (red line) of the (D^0, X_A) line of the GaN NW ensemble recorded at 5 K with a spectral resolution of 1 meV. The dotted lines correspond to single exponential functions with decay times of 170 and 600 ps. The black line is a fit described in the text. Inset: Histogram of the radius R for about 4400 NWs with a fit to a gamma distribution (red line). (b) PL transients of the GaN NW ensemble for different temperatures of 4 (cyan), 5 (red), 10 (blue), 15 (magenta), 20 (green), and 30 K (black).

agreement with literature values for unstrained GaN.[10,11] In order to map out the location of the individual light-emitting NWs, we generated maps of the PL intensity in the region close to the edge of the wafer. Figure 2(b) shows three representative time-integrated PL spectra of NWs labeled NW1, NW2, and NW3 recorded for pulsed excitation at different locations identified by the mapping. Note that the PL spectra of the three individual NWs are clearly different. This finding is true for most individual NWs measured in the region near the edge of the NW wafer. The spectra of NW1 and NW2 are dominated by the (D^0, X_A) line and a shoulder at about 3.476 eV (dashed line), which we attribute to the exciton bound to a surface donor $(D^0, X_A)_S$, while the spectrum of NW3 consists of only one peak at 3.469 eV.[11]

The PL transients of the three NWs in Fig. 2(b) have been recorded using an energy fluence $\rho_E = 92$ nJ cm^{-2}. These transients spectrally integrated over the whole PL band are displayed in Fig. 3(a) on a logarithmic intensity scale. Note that the hump at about 500 ps is a result of the system's response function (SRF). Once the SRF is taken into account by convolution, the decay of all three NWs can be fit by a single exponential function with very different time constants of 98, 287, and 349 ps for NW1, NW2, and NW3, respectively. Note that NW1 experiences the fastest decay of the three NWs displayed in Fig. 3(a), which is consistent with the presence of the $(D^0, X_A)_S$ exciton in the PL spectrum of NW1 as indicated in Fig. 2(b) and the correspondingly stronger influence of nonradiative surface recombination. In general, the measured time constants of the individual NWs vary between 50 and 400 ps. With increasing temperature, the transients remain single exponential, as shown in Fig. 3(b) for NW3 in the temperature range from 5 to 30 K, again on a logarithmic intensity scale. The decay time continuously decreases with increasing temperature from 349 to 57 ps, which reflects an increasing contribution of nonradiative recombination. In fact, the spectrally integrated intensity of the PL emission from the NW ensemble decreases by a factor of 4, when the temperature is increased from 4 to 30 K.

In the following, we will compare the single exponential PL transient of an individual NW with the time dependence of the PL response of the NW ensemble of Fig. 2(a). The PL transient in Fig. 4(a) has been obtained by spectrally integrating over a narrow range of the (D^0, X_A) line of the NW ensemble and detecting the corresponding signal by TCSPC. Note again that the hump at about 500 ps is due to the SRF. The transient of the NW ensemble clearly exhibits a nonexponential time dependence with characteristic times between 170 and 600 ps, as indicated by the dotted lines in the semilogarithmic plot of Fig. 4(a). The transient in Fig. 4(a) was recorded using an energy fluence $\rho_E = 18$ nJ cm^{-2}, i.e., similar to the value used for the single NW transients in Fig. 3. Note that the same behavior is also

observed for values of ρ_E two orders of magnitude smaller. We also measured the PL transients of the NW ensemble for different temperatures between 4 and 30 K, the results of which are shown in Fig. 4(b), using again a logarithmic intensity scale. All transients remain nonexponential. With increasing temperature, the transients exhibit faster decays due to a stronger contribution of nonradiative recombination.

In the following, we analyze the PL transient of the NW ensemble shown in Fig. 4(a) based on the observation that individual NWs exhibit single exponential PL transients with different decay times. In principle, the PL transient of the NW ensemble should be described by a superposition of 1500 single exponential components. Clearly, the actual determination of the corresponding individual decay times is impractical. Since we attribute the different observed decay times for single NWs to an impact of nonradiative surface recombination, the area A of the cross section for about 4400 NWs in the central part of the wafer was determined using top-view SEM images in order to estimate the surface-to-volume ratio. The histogram displayed in the inset of Fig. 4(a) shows the equivalent disk radius $R = \sqrt{A/\pi}$ of the NWs. The histogram can be approximated by the gamma distribution $\Gamma(R)$.[12] A fit to the data in the inset of Fig. 4(a) indicated by the red line yields a value for the average radius of $R_a = 30$ nm and a variance of $\sigma = 15$ nm. $\Gamma(R)$ provides a continuous expression for the probability of finding a NW with a radius R.

To extract quantitative information from the transient in Fig. 4(a), we developed a straightforward model based on the above assumption that the cross section of the NW is approximately circular and can be described by R. Furthermore, we assume that an exciton bound to a donor located at a distance $r < (R - L)$ from the center of the NW experiences the bulk recombination rate γ_b, while for values of r in the range of $(R - L) < r < R$ the rate $\gamma(r)$ increases linearly to γ_s, the surface recombination rate. Here, L parametrizes the spatial extent of the outer shell of the NW, in which nonradiative surface recombination can influence the recombination rate of the (D^0, X_A) transition. In order to avoid having to explicitly account for each randomly placed (D^0, X_A) exciton with its corresponding value of $\gamma(r)$, we integrate $\gamma(r)$ over r, which for $L < R$ becomes approximately $\gamma(R) = \gamma_b + (\gamma_s - \gamma_b)\frac{L}{R}$. By introducing an effective surface recombination velocity $\tilde{S} = (\gamma_s - \gamma_b)L/2$, it follows that $\gamma(R) = \gamma_b + 2\tilde{S}/R$. This expression formally resembles the usual expression for the surface recombination of free excitons.[13] Note that $\gamma(R)$ corresponds to a type of mean value, which would be observed by averaging over several NWs with the same radius R. The PL intensity transient $I(t)$ of the (D^0, X_A) line of the ensemble can thus be described by the convolution of $\Gamma(R)$ with a single exponential decay,

$$I(t) = I_0 \int_0^\infty \Gamma(R) \exp[-\gamma(R)t] dR,$$

with three parameters γ_b, $\tilde{S}$, and I_0, where I_0 denotes the maximum intensity. A fit of this equation to the data in Fig. 4(a) including the convolution with the SRF yields the following values for $\tilde{S} = (6.32 \pm 0.15) \times 10^3$ cm/s and $1/\gamma_b = (5500 \pm 2500)$ ps. The decay is mainly determined by the surface recombination, since the term $R/2\tilde{S}$ for the largest NWs with a radius of 75 nm corresponds to a time constant of about 600 ps, which is about a factor of 2–3 smaller than the longest decay times reported in the literature.[14,15] Therefore, the one order of magnitude larger value of $1/\gamma_b$ compared to $R/2\tilde{S}$ for the largest NWs is of limited significance. The value of $\tilde{S}$ obtained for bound excitons at low temperatures is a factor of 1.5 smaller than the reported value for free excitons at room temperature for GaN NWs[13] with a diameter one order of magnitude larger than that of our NWs. It is about one order of magnitude smaller than $S \approx 4 \times 10^4$ cm/s found for free excitons in GaN epilayers,[16] where the surface is formed by the polar C plane, while in the NWs the surfaces correspond to nonpolar M planes. However, the fit underestimates the transient for $t > 1.5$ ns, which may be a result of the applied approximations. In addition, the assignment of an average value of $\gamma(R)$ to a NW with a diameter R, which may contain more than one (D^0, X_A) exciton at different locations r so that it would already exhibit a time dependence with more than one time constant, may not be sufficiently accurate.

In conclusion, we have detected the PL transients of individual free-standing GaN NWs, which exhibit single exponential decays with individual decay times at 5 K. This single exponential decay is preserved up to sample temperatures of at least 30 K. In addition, the time-integrated PL spectra are also characteristic for each individual NW. In contrast, the PL transients of the NW ensemble always exhibit a nonexponential decay, independent of the excitation intensity and temperature (up to 30 K). The nonexponential time dependence of the PL transient of the NW ensemble can be explained by a superposition of the responses from the different individual NWs, each exhibiting a single exponential decay with a different decay time. We applied a model taking nonradiative surface recombination into account by introducing an effective surface recombination velocity $\tilde{S}$. The fits to our data reveal that nonradiative surface recombination essentially dominates the PL transients of these ultrathin NWs. In general, we can neither control the position of the donor nor the surface-to-volume ratio of the nanowire. However, since the transition energy depends on the distance of the donor from the surface, it would be interesting to study the dependence of the decay time as a function of the transition energy for different single nanowires.

The authors would like to thank A. Bluhm for recording some of the SEM images.

*flissi@pdi-berlin.de

[1] A. Kikuchi, M. Kawai, M. Tada, and K. Kishino, Jpn. J. Appl. Phys., Part 2 **43**, L1524 (2004).

[2] W. Guo, M. Zhang, A. Banerjee, and P. Bhattacharya, Nano Lett. **10**, 3355 (2010).

[3] H.-W. Lin, Y.-J. Lu, H.-Y. Chen, H.-M. Lee, and S. Gwo, Appl. Phys. Lett. **97**, 073101 (2010).

[4] J. S. Wright, W. Lim, D. P. Norton, S. J. Pearton, F. Ren, J. L. Johnson, and A. Ural, Semicond. Sci. Technol. **25**, 024002 (2010).

[5] C. M. Lieber and Z. L. Wang, MRS Bull. **32**, 99 (2007).

[6]J. A. Czaban, D. A. Thompson, and R. R. LaPierre, Nano Lett. **9**, 148 (2009).

[7]L. Geelhaar, C. Chèze, B. Jenichen, O. Brandt, C. Pfüller, S. Münch, R. Rothemund, S. Reitzenstein, A. Forchel, T. Kehagias, P. Komninou, G. P. Dimitrakopulos, T. Karakostas, L. Lari, P. R. Chalker, M. H. Gass, and H. Riechert, IEEE J. Sel. Top. Quantum Electron. **17**, 878 (2011).

[8]C. Pfüller, O. Brandt, T. Flissikowski, C. Chèze, L. Geelhaar, H. T. Grahn, and H. Riechert, Nano Res. **3**, 881 (2010).

[9]C. Pfüller, O. Brandt, F. Grosse, T. Flissikowski, C. Chèze, V. Consonni, L. Geelhaar, H. T. Grahn, and H. Riechert, Phys. Rev. B **82**, 045320 (2010).

[10]M. A. Reshchikov and H. Morkoç, J. Appl. Phys. **97**, 061301 (2005).

[11]O. Brandt, C. Pfüller, C. Chèze, L. Geelhaar, and H. Riechert, Phys. Rev. B **81**, 045302 (2010).

[12]*NIST/SEMATECH e-Handbook of Statistical Methods*, edited by C. Croarkin and P. Tobias (NIST/SEMATECH, 2010), Chap. 1.3.6.6.11, http://www.itl.nist.gov/div898/handbook/.

[13]J. B. Schlager, K. A. Bertness, P. T. Blanchard, L. H. Robins, A. Roshko, and N. A. Sanford, J. Appl. Phys. **103**, 124309 (2008).

[14]Y. C. Zhong, K. S. Wong, W. Zhang, and D. C. Look, Appl. Phys. Lett. **89**, 022108 (2006).

[15]B. Monemar, P. P. Paskov, J. P. Bergman, G. Pozina, A. A. Toropov, T. V. Shubina, T. Malinauskas, and A. Usui, Phys. Rev. B **82**, 235202 (2010).

[16]R. Aleksiejūnas, M. Sūdžius, T. Malinauskas, J. Vaitkus, K. Jarašiūnas, and S. Sakai, Appl. Phys. Lett. **83**, 1157 (2003).